Transient spatiotemporal chaos is extensive in three reaction-diffusion networks

Dan Stahlke* and Renate Wackerbauer†
Department of Physics, University of Alaska, Fairbanks, Alaska 99775-5920, USA
(Received 5 August 2009; published 24 November 2009)

Extensive (asymptotic) spatiotemporal chaos is comprised of statistically similar subsystems that interact only weakly. A systematic study of transient spatiotemporal chaos reveals extensive system behavior in all three reaction-diffusion networks for various boundary conditions. The Lyapunov dimension, the sum of positive Lyapunov exponents, and the logarithm of the transient lifetime grow linearly with the system size. The unstable manifold of the chaotic saddle has nearly the same dimension as the saddle itself, and the stable manifold is nearly space filling.

DOI: 10.1103/PhysRevE.80.056211 PACS number(s): 05.45.Jn

I. INTRODUCTION

Transient spatiotemporal chaos is a generic pattern in extended nonequilibrium systems in which spatiotemporal dynamics spontaneously changes from chaotic to regular (steady-state or periodic) behavior. Transient spatiotemporal chaos was found in models for semiconductor charge transport [1], for the CO oxidation on single-crystal Pt surfaces [2], for a cubic autocatalytic reaction [3], in models of turbulent dynamics [4,5], and in systems of coupled logistic maps [6,7]. Experimental studies show that turbulence in shear flow is transient [8]. "Stable chaos" (with a negative Lyapunov exponent) is transient in systems of coupled one-dimensional maps [9].

Extended chaotic systems that have no long-range interactions are expected to be uncorrelated at large length scales and therefore should behave as a sum of their parts [10]. Then spatiotemporal chaos is extensive, and the spectrum of Lyapunov exponents converges to a function that is intensive. This implies that the attractor dimension (Lyapunov dimension) grows in direct proportion to the volume of the system [11,12]. While extensivity in (asymptotic) spatiotemporal chaos has been studied for a while [11–16], extensivity in transient spatiotemporal chaos is rather unexplored [2,17].

The average lifetime of transient spatiotemporal chaos typically grows exponentially with the volume of the system [3,18,19]. The origin of this exponential scaling is most likely due to the probability for randomly uncorrelated regions generating a global pattern that initiates the collapse of spatiotemporal chaos [1,17,20]. This feature of transient spatiotemporal chaos particularly motivates more detailed studies on extensive properties in transient dynamics.

This paper systematically explores and verifies extensivity of transient spatiotemporal chaos in three reaction-diffusion networks and a variety of boundary conditions. Section II introduces the three excitable reaction-diffusion networks with Gray-Scott (GS) [21], Bär-Eiswirth (BE) [22], and Wacker-Schöll (WS) [1] reaction dynamics. The lifetime of transient spatiotemporal chaos is discussed in Sec. III, and the Lyapunov spectra and dimensions are investigated in Sec. IV. Section V describes dimensional properties of the chaotic saddle, and Sec. VI focuses on various densities and their qualitative statistical interpretations.

II. REACTION-DIFFUSION NETWORKS

The networks consist of N diffusively coupled, identical, and continuous-time dynamical elements. At each network node n $(n=1,2,\ldots,N)$ the uncoupled dynamics is given by $d\mathbf{x}_n/dt=\mathbf{F}(\mathbf{x}_n)$ with $\mathbf{x}_n$ as a d-dimensional state vector. The reaction-diffusion network is given by

$$\frac{d\mathbf{x}_n}{dt}=\mathbf{F}(\mathbf{x}_n)+D\sum_{j=1}^{N}G_{nj}H\mathbf{x}_j. \tag{1}$$

D is a global coupling parameter. H is a $d\times d$ diagonal matrix representing the relative diffusion of each species. G is an $N\times N$ symmetric Laplacian matrix required to meet the condition $\Sigma_{j=1}^{N}G_{ij}=0$. For a regular network in one dimension the coupling matrix G is

$$G_{ij}=\nabla_{ij}^2=\delta_{i,j-1}-2\delta_{ij}+\delta_{i,j+1}, \tag{2}$$

with $i,j=1,2,\ldots,N$. The indices are equivalent modulo N for periodic boundary conditions and $G_{i1}=\delta_{i2}-\delta_{i1}$ and $G_{iN}=\delta_{i,N-1}-\delta_{iN}$ for no-flux boundary conditions. In the presence of a single shortcut of length k between node 1 and $k+1$ the coupling matrix becomes

$$G_{ij}=\nabla_{ij}^2+\delta_{i1}(\delta_{j,k+1}-\delta_{ij})+\delta_{i,k+1}(\delta_{j1}-\delta_{ij}). \tag{3}$$

The coupling strength parameter D controls the characteristic length scale. From the rescaling of Eq. (1) it follows that the general characteristics of the system remain the same if N and D are both increased while holding $N/\sqrt{D}$ constant. If N goes to infinity with $N/\sqrt{D}$ held constant the system approaches a continuous form. On the other hand if N (and hence D) is made too small discretization effects will start to become significant and eventually the system will no longer be able to support chaos. In this paper D is large enough for the networks to be good approximations for the continuum system, except where noted otherwise.

We consider three excitable dynamical systems F: the GS [21], the BE [22], and the WS [1] systems. Each of the systems consists of two species $(d=2)$, so each $\mathbf{x}_n$ is a two-

*dstahlke@gmail.com
†rawackerbauer@alaska.edu

dimensional vector. Thus, the uncoupled system does not exhibit chaos, and spatiotemporal chaos is induced by the diffusive coupling of the excitable dynamical elements in Eq. (1).

The *Gray-Scott system* [21] represents an open autocatalytic reaction $A+2B \rightarrow 3B$ and $B \rightarrow C$. The equations are

$$\mathbf{F}\left(\begin{bmatrix} a \\ b \end{bmatrix}\right) = \begin{bmatrix} 1-a-\mu ab^2 \\ \mu ab^2 - \Phi b \end{bmatrix}, \quad H = \begin{bmatrix} 1 & 0 \\ 0 & 1 \end{bmatrix}, \tag{4}$$

where a and b are dimensionless species concentrations and ϕ and μ are bifurcation parameters. In the parameter regime of coupling-induced spatiotemporal chaos the function $\mathbf{F}$ has three fixed points: $S^n=(1,0)$ is a stable node that exists for all values of ϕ and μ, and the additional fixed points $S^f=([1-\sqrt{1-4\phi^2/\mu}]/2,[1+\sqrt{1-4\phi^2/\mu}]/2\phi)$ and $S^s=([1+\sqrt{1-4\phi^2/\mu}]/2,[1-\sqrt{1-4\phi^2/\mu}]/2\phi)$ exist for values of μ above the saddle node bifurcation point $\mu_{sn}=4\phi^2$. When $\mu > \mu_{sn}$, S^s is a saddle point and within the range $2<\phi<4$, S^f is an unstable focus for values of μ below the subcritical Hopf bifurcation point $\mu_H=\phi^4/(\phi-1)$. The parameter range $[\mu_c,\mu_H]$ yields wave-induced spatiotemporal chaos, with μ_c being the critical threshold for traveling-wave solutions [3]. For $\phi=2.8$, $\mu_c \approx 33$ and $\mu_H \approx 34.1$. In the Gray-Scott network [Eqs. (1) and (4)] the spatiotemporal chaos is ŠIlnikov-like; a typical trajectory at a network node spirals away from the unstable focus toward the stable node and then is reinjected into the neighborhood of the unstable focus by the propagating reaction-diffusion front [23]. For the calculations in this paper we have used the parameters $\mu \in \{33.5,33.7,33.9\}$ and $\Phi=2.8$.

The *Bär-Eiswirth system* [22] describes a surface reaction model for the oxidation of CO on Pt and is given by

$$\mathbf{F}\left(\begin{bmatrix} a \\ b \end{bmatrix}\right) = \begin{bmatrix} \frac{a}{\epsilon}(1-a)\left(a-\frac{b+\beta}{\alpha}\right) \\ f(a)-b \end{bmatrix}, \quad H = \begin{bmatrix} 1 & 0 \\ 0 & 0 \end{bmatrix}, \tag{5}$$

and

$$f(a) = \begin{cases} 0 & \text{if } a < 1/3 \\ 1-6.75a(a-1)^2 & \text{if } 1/3 \le a \le 1 \\ 1 & \text{if } a > 1. \end{cases}$$

a represents the activator concentration and b represents the inhibitor concentration. α, β, and ϵ are bifurcation parameters, with ϵ determining the difference in time scale between the slow variable b and the fast variable a. In the parameter regime of coupling-induced spatiotemporal chaos the function $\mathbf{F}$ has three relevant fixed points: a stable node $S^n=(0,0)$, a saddle point $S^s=(\frac{\beta}{\alpha},0)$, and an unstable focus which must be computed numerically. Additional fixed points at (1,1) and $(\frac{1+\beta}{\alpha},1)$ are not relevant to the region of phase space in which chaos exists [18]. In the Bär-Eiswirth network [Eqs. (1) and (5)] a backfiring instability is reported to be the origin of spatiotemporal chaos; the traveling pulses become unstable to allow re-excitation behind the pulse to create new pulses [22,24,25]. In this paper we use the parameters $\alpha=0.84$, $\beta=0.07$, and $\epsilon=0.12$.

The *Wacker-Schöll system* [1] describes charge transport in a simplified model of layered semiconductors and is given by

$$\mathbf{F}\left(\begin{bmatrix} a \\ b \end{bmatrix}\right) = \begin{bmatrix} \frac{b-a}{(b-a)^2+1} - \tau a \\ \alpha[j_0-(b-a)] \end{bmatrix}, \quad H = \begin{bmatrix} 1 & 0 \\ 0 & d \end{bmatrix}, \tag{6}$$

where a represents the interface charge density and b represents the dimensionless voltage [1]. The bifurcation parameter j_0 represents normalized external current, α determines the time scale of the system, d is an effective diffusion constant, and τ is an internal system parameter [26]. In the parameter regime of coupling-induced spatiotemporal chaos the function $\mathbf{F}$ has an unstable focus at $(j_0/[(j_0^2+1)\tau], j_0+j_0/[(j_0^2+1)\tau])$ and a stable limit cycle. In the Wacker-Schöll network [Eqs. (1) and (6)] a Hopf bifurcation as temporal instability and a Turing bifurcation as diffusive instability cause the irregular spatiotemporal spiking pattern in spatiotemporal chaos [26]. We use the parameters $\alpha=0.02$, $\tau=0.05$, $j_0=1.21$, and $d=8$, for which the system is near a codimension-2 Turing-Hopf bifurcation point.

All of these three dynamical systems have an excitable attractor (either node or limit cycle) such that strong enough stimuli can cause large excursions from the attractor. In the BE and GS systems the stable manifold of the saddle acts like a separatrix between excited states and states of immediate return to the attractor. In the WS system the limit cycle is attracting but not Lyapunov stable. Its excitation cycles grow continuously with increasing perturbation from the limit cycle, and their size is large in comparison to the limit cycle already for small perturbations from the limit cycle. In all three systems, spatiotemporal chaos is introduced by diffusive coupling, and regular attractors are accessible in the case of the spatially homogeneous system. These systems differ in their coupling as the GS system has equal diffusivities, the BE system has zero diffusivity for one species, and the WS system has a diffusion-driven Turing instability. The bifurcation scenario for the uncoupled systems is also different: the GS system, Eq. (4), reaches the parameter regime of spatiotemporal chaos, in which there is no limit cycle present, via a subcritical Hopf bifurcation; the BE system, Eq. (5), reaches the parameter regime of spatiotemporal chaos, in which there is no limit cycle present, via a supercritical Hopf bifurcation that generates an unstable focus and a stable limit cycle, which disappears via a saddle loop bifurcation; in the parameter regime of spatiotemporal chaos the WS system has a stable limit cycle that is generated via a supercritical Hopf bifurcation.

III. LIFETIME OF TRANSIENT SPATIOTEMPORAL CHAOS

Earlier studies have reported that spatiotemporal chaos is transient in the one-dimensional WS [1], the two-dimensional BE [2], and the one- and two-dimensional GS [3] models. After a regime of sustained spatiotemporal chaos with a rapid decay of spatial correlations and a positive largest Lyapunov exponent, the systems exhibit a spontaneous

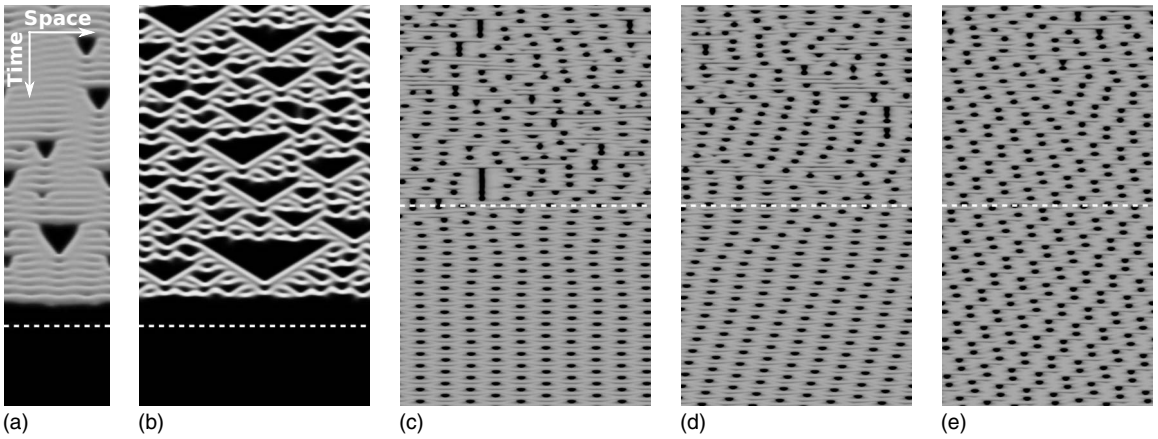

FIG. 1. Spatiotemporal pattern of the variable a during the collapse of spatiotemporal chaos for (a) the GS system (μ=33.7, Φ=2.8, D=16, N=210, and 240 time units shown), (b) the BE system (α=0.84, β=0.07, ϵ=0.12, D=16, N=200, and 240 time units shown), and (c)–(e) the WS system (α=0.02, τ=0.05, j_0=1.21, d=8, D=0.25, and 24 000 time units shown) with different network sizes [N=500 in (c), N=460 in (d), and N=420 in (e)]. The dotted line represents the time of collapse as determined by our algorithm, with the transient lifetimes (a) T=4 574 539, (b) T=3 600 582, (c) T=24 794, (d) T=491 481, and (e) T=32 531. The pattern in (c) was observed often, with the initial wavy distortions from periodicity disappearing for large simulation times. The patterns in (d) and (e) were less common. In (d) the asymptotic state is rotated in space and time, which allows a spatial period that is a half-integer fraction of the system size [27]. The numerical integration used periodic boundary conditions and a fourth-order Runge-Kutta integration method with a numerical integration time step of Δt=0.003 for the GS and BE systems and Δt=0.03 for the WS system.

system intrinsic collapse to a regular state [Figs. 1(a)–1(e)]. Such a sudden collapse points to the coexistence of a chaotic saddle with the regular attractor(s) [17].

For the GS and the BE systems spatiotemporal chaos collapses to a spatially homogeneous stable steady state, in which the dynamics at each network node reaches the asymptotic stable steady state S^n of the uncoupled system. This spatially homogeneous state represents the attractor on the synchronization manifold [18] in Eq. (1). For both systems the transient spatiotemporal chaotic pattern is characterized by an irregular distribution of black patches, in which trajectories of neighboring network nodes approach the stable steady state S^n of the homogeneous system [Figs. 1(a) and 1(b)] together. In the WS system the transient pattern is characterized by an irregular spiking [Figs. 1(c)–1(e)]. The lighter color corresponds to trajectories of neighboring network nodes being closer to the stable limit cycle of the homogeneous system, whereas the dark spots correspond to neighboring trajectories away from the stable limit cycle. Our simulations showed that the asymptotic regular state was periodic in time with various spatial shifts [27].

Transient spatiotemporal chaos is often characterized by the rate at which an ensemble of systems with different initial conditions collapses [1,2,17], since the transient dynamics can be very long lived. We calculate the average lifetime $\langle T\rangle$ for transient spatiotemporal chaos explicitly for all three systems. For the Gray-Scott and the Bär-Eiswirth systems, spatiotemporal chaos only collapsed to the stable node on the synchronization manifold, and the lifetime T of transient spatiotemporal chaos is determined from

$$T = \inf_t \left\{ \max_n \left\| \mathbf{x}_n(t) - \sum_m \frac{\mathbf{x}_m(t)}{N} \right\|_\infty < 10^{-6} \right\},$$

where $\|\cdot\|_\infty$ denotes the maximum norm over the components of $\mathbf{x}$. Transient spatiotemporal chaos in the Wacker-Schöll system always collapsed into a periodic asymptotic state, and the lifetime T is determined by tracking a (finite time) maximum Lyapunov exponent [28]. When the maximum Lyapunov exponent—averaged over a gliding window of 150 000 time units—drops below zero, the system is deemed to have reached a nonchaotic state starting at the beginning of the window [29].

Figures 2(a)–2(c) show that the average transient lifetime $\langle T\rangle$ of spatiotemporal chaos increases exponentially with the network size N for all three systems. Hence, $\ln\langle T\rangle$ is an extensive quantity. The rate at which $\ln\langle T\rangle$ increases with N (slope of the linear fit in Fig. 2) depends on the boundary conditions, which is consistent with earlier studies on the Gray-Scott system [3,18,30] and similar to results for the two-dimensional Bär-Eiswirth system [2]. If only the larger values of N are considered the slopes are quite similar to each other and it is possible that they converge as $N\to\infty$. For example, if only data points for $\langle T\rangle > 10^5$ are fitted the slopes for periodic and no-flux boundary conditions agree to within 10% for the Gray-Scott model, which is similar to how much the slopes change when shifting the cutoff from $\langle T\rangle > 10^4$ to $\langle T\rangle > 10^5$.

This independence of the slopes from boundary conditions is supported from a qualitative argument. Exponential scaling of the average lifetime with the network size N arises if a system is comprised of weakly interacting and statistically uncorrelated units of length ξ. If P is the probability for a unit ξ to be conducive to loss of chaos at any moment of time, then spatiotemporal chaos collapses with the probability $P^{N/\xi}$, when all units are in a state conducive to collapse [17,20]. The logarithm of the average lifetime is then $\ln\langle T\rangle \sim (-N/\xi)\ln P$. If a boundary condition changes the probability for collapse in one of the units to Q [31], then the logarithm of the average lifetime would be $\ln\langle T\rangle \sim -\ln[QP^{(N/\xi-1)}] = (-N/\xi)\ln P - \ln(Q/P)$, which does not af-

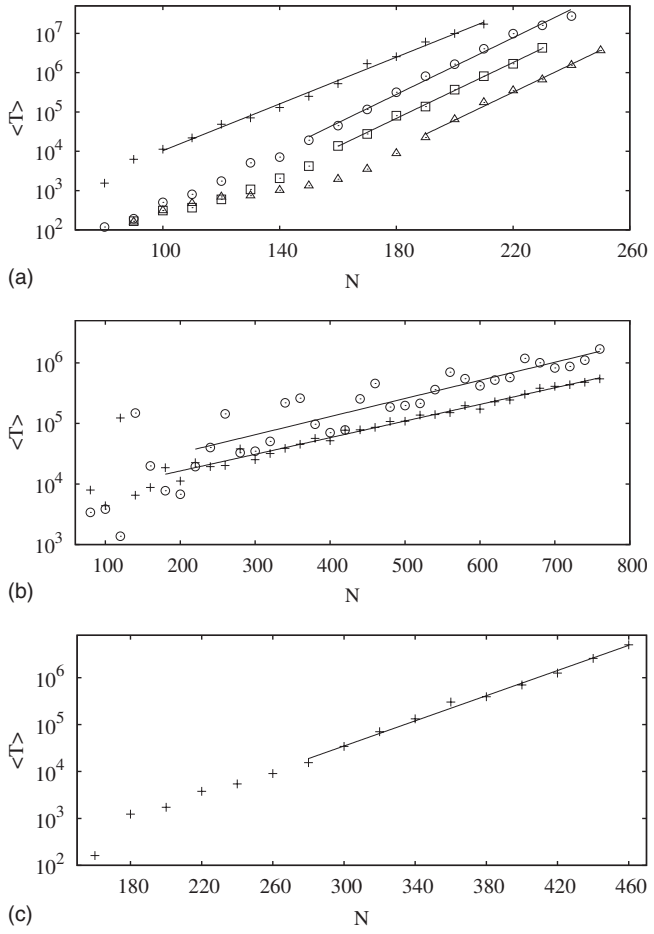

FIG. 2. Average transient lifetime $\langle T\rangle$ versus number of network nodes N for (a) the Gray-Scott, (b) the Wacker-Schöll, and (c) the Bär-Eiswirth systems. Various boundary conditions were used, including no flux (+), periodic (○), periodic with shortcut of length 50 (□), and periodic with shortcut of length $N/2$ (△). Each data point was determined from at least 104 random initial conditions. The error bar (1 standard deviation, not plotted here) for each data point is on the order of $\langle T\rangle$ [18]. The lines show least-squares linear fits of the average transient lifetimes. The linear fit includes the range of network sizes N for which the average lifetime was consistently greater than 10^4, in order to exclude artifacts from the exaggerated significance of boundary conditions for small N. The lifetimes for small N can also be affected by the initial transient before the chaotic saddle is reached. All the other parameters and simulation procedures are the same as in Fig. 1.

fect the slope. This line of reasoning is of course valid only if $Q\neq 0$ [32].

Figure 2(b) also reveals that $\ln\langle T\rangle$ shows significant deviation from extensivity in the Wacker-Schöll system, especially for smaller network sizes N and periodic boundary conditions. As the number of nodes increases the oscillations of $\ln\langle T\rangle$ around the linear fit decrease in amplitude and match more closely the expected extensivity. One possible explanation for the deviation from extensivity is that spatial period must be an integer multiple of network size. This hypothesis is supported by the fact that the most commonly observed asymptotic pattern [1] as well as the oscillation of the deviation from extensivity of $\ln\langle T\rangle$ both have a spatial

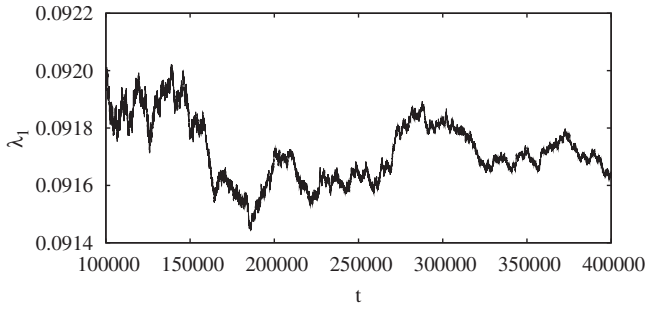

FIG. 3. Convergence behavior of the largest (finite time) Lyapunov exponent λ_1 for the Gray-Scott system with simulation time t. This convergence behavior is typical for Lyapunov exponents in all three models. The error is estimated by computing the maximum difference between the final value and any value from the second half of the simulation.

period of approximately 100 nodes. For larger networks the deviation from extensivity decreases since it becomes easier to approximate any given spatial period with an integer fraction of the network size.

An earlier study showed for the Gray-Scott system that the average lifetime is related to the number of unstable transverse modes along a typical trajectory within the synchronization manifold [18]. The number of unstable transverse modes as well as $\ln\langle T\rangle$ are extensive quantities. Both quantities increase linearly with the network size for a given coupling strength D, and they both increase linearly with $1/\sqrt{D}$ for a given network size N.

IV. LYAPUNOV SPECTRUM AND RELATED QUANTITIES

Measures that quantify chaotic attractors can also characterize chaotic saddles (transient spatiotemporal chaos) for large network sizes if the lifetimes are long enough for the measures to converge. The Lyapunov spectra for the reaction-diffusion networks in Eq. (1) were computed numerically [33] from infinitesimal displacement vectors $\mathbf{y}_n$ about $\mathbf{x}_n$ that evolve according to $\partial\mathbf{y}_n/\partial t=J|_{\mathbf{x}_n}\mathbf{y}_n+D\Sigma_{j=1}^{N}G_{nj}H\mathbf{y}_j$, where $J|_{\mathbf{x}_n}$ is the Jacobian of $\mathbf{F}$ evaluated at $\mathbf{x}_n$. With periodic Gram-Schmidt orthonormalization of the $\mathbf{y}_n$ vectors every T_{rn} time units and with the logarithm of the corresponding normalization coefficients being added to a running tally β_i, the (finite time) Lyapunov exponents are given by β_i/t for any time t [33]. Fourier modes were used as initial perturbations, although the choice of initial perturbation should have little effect on the final result [33]. A renormalization interval of $T_{rn}=3$ time units was used in all cases, and simulation times varied between 2.8×10^5 and 5.6×10^6 time units. The Lyapunov spectra were robust to changes in renormalization interval and integration time step [34]. Some of the systems collapsed into a steady or periodic state part way through the simulation [35]. If the largest Lyapunov exponent for a gliding window of length 3000 time units fell below zero, all samples after the beginning of this window were discarded. Figure 3 shows a typical convergence behavior of a Lyapunov exponent; it happens slowly. The convergence error was estimated as the maxi-

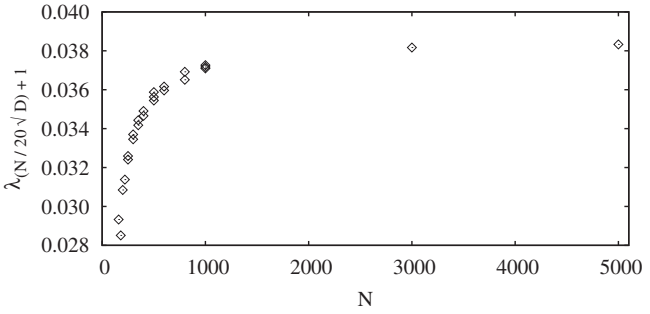

FIG. 4. The scaled index Lyapunov exponent $\lambda_{N/(20\sqrt{D})+1}$ vs network size N for the Gray-Scott system. Lyapunov exponents are indexed starting from λ_1, and linear interpolation is used in cases where the index $i=N/20\sqrt{D}+1$ is not an integer. The multiple data points for certain values of N correspond to different initial conditions and are close together. All the other parameters are the same as in Fig. 1(a).

mum difference between the final (finite time) Lyapunov exponent and any intermediate value from the second half of the simulation.

Spatiotemporal chaos is said to be extensive if the spectrum of Lyapunov exponents λ_i converges to a function $f(i/N)$ that is intensive. This implies that the attractor dimension increases in proportion to the system size N and that a dimension density exists [11]. We will show that transient spatiotemporal chaos also fulfills these criteria for all three models.

Figure 4 shows a *single Lyapunov exponent* λ_i for each network size N, with the index $i=N/20\sqrt{D}+1$ scaled in proportion to the network size N. $\lambda_{N/(20\sqrt{D})+1}$ converges with N in good approximation. This behavior is consistent with the spectrum of Lyapunov exponents converging to a function that is intensive, and with the existence of a Lyapunov spectrum density. Qualitatively similar convergence behavior was found for the Lyapunov spectrum in the Bär-Eiswirth model and in the Wacker-Schöll model.

The *Lyapunov dimension* ($D_{\mathcal{L}}$) is conjectured to be equal to the information dimension for typical attractors [36]; it is defined as

$$D_{\mathcal{L}} = j + \frac{\lambda_1 + \cdots + \lambda_j}{|\lambda_{j+1}|}, \tag{7}$$

where j is the largest integer for which $\Sigma_{i=1}^{j}\lambda_i > 0$. For chaotic saddles the information dimension has a correction term proportional to the escape rate, which is negligible for large enough system sizes such as those considered in this paper [37].

Figure 5(a) shows that the Lyapunov dimension $D_{\mathcal{L}}$ increases linearly with the network size N for all three reaction-diffusion network models with varying system parameters. The deviation of the $D_{\mathcal{L}}$ values from linearity was small for all systems studied; a representative example for the Gray-Scott system is given in Fig. 5(b). These findings indicate that $D_{\mathcal{L}}$ is an extensive quantity during the transient phase of spatiotemporal chaos. Extensive transient spatiotemporal chaos in these models was also found for various boundary conditions, including periodic and no-flux boundary conditions as well as periodic with the presence of shortcuts in the network. The results are summarized in Table I.

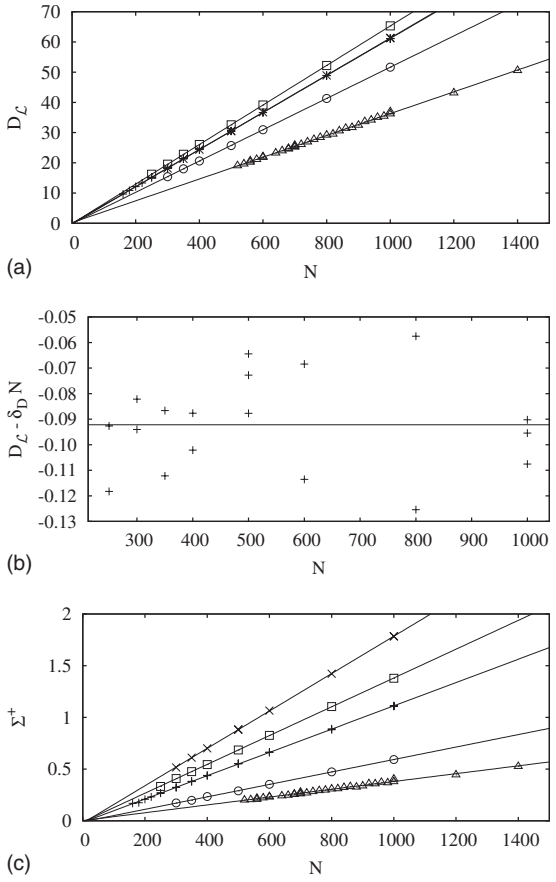

FIG. 5. (a) Lyapunov dimension $D_{\mathcal{L}}$ versus network size N for five systems with periodic boundary conditions: Bär-Eiswirth model with $\alpha=0.84$, $\beta=0.07$, $\epsilon=0.12$, and $D=16$ ($\times$); Gray-Scott model ($\phi=2.8$, $D=16$) with $\mu=33.5$ ($\square$), $\mu=33.7$ (+), and $\mu=33.9$ ($\bigcirc$); and Wacker-Schöll model with $\alpha=0.02$, $\tau=0.05$, $j_0=1.21$, $d=8$, and $D=0.25$ ($\triangle$). The Lyapunov dimension for the Bär-Eiswirth model ($\times$) and the Gray-Scott model ($\mu=33.7$, +) have very similar values, making them hard to distinguish in the graph, although their Lyapunov spectra are different. The full lines correspond to a least-squares linear fit of the corresponding data points. The error for each data point, not plotted in the figure, was estimated by computing the maximum difference between the final value of $D_{\mathcal{L}}$ and any intermediate value from the second half of the simulation; errors were smaller than 2.5% of the data point values and typically less than 0.3% for Gray-Scott and Bär-Eiswirth systems. (b) Deviation of $D_{\mathcal{L}}$ values from the linear fit in (a) for the Gray-Scott system with $\mu=33.7$. For this system $D_{\mathcal{L}}$ was calculated for different initial conditions for each network size N to estimate the convergence behavior. These data points were plotted in both figures, (a) and (b), but they are too close to be distinguished in (a). The horizontal line represents the y intercept of the linear fit, which was not subtracted when plotting deviation from the linear trend. (c) Sum of positive Lyapunov exponents Σ^+ versus network size N for the same systems as in (a). The values for the Wacker-Schöll system have been multiplied by 20 to improve clarity.

The *sum of positive Lyapunov exponents* (Σ^+) represents an upper bound for the Kolmogorov-Sinai entropy [36]. For chaotic saddles this upper bound can be refined by subtract-

TABLE I. Summary of Lyapunov dimension $D_{\mathcal{L}}$ and sum of positive Lyapunov exponents Σ^+ for the Bär-Eiswirth (BE) model ($\alpha=0.84$, $\beta=0.07$, $\epsilon=0.12$), the Gray-Scott (GS) model ($\mu \in \{33.5, 33.7, 33.9\}$, $\Phi=2.8$), and the Wacker-Schöll (WS) model ($\alpha=0.02$, $\tau=0.05$, $j_0=1.21$, $d=8$) for different system parameters and different boundary conditions. A least-squares linear fit was made for $D_{\mathcal{L}}$ and Σ^+ versus network size N, and a least-squares linear fit was made for $D_{\mathcal{L}}$ and Σ^+ versus $1/\sqrt{D}$ with coupling parameter D. A least-squares constant fit was done for $D_{\mathcal{L}}$ and Σ^+ for fixed effective system sizes $N/\sqrt{D}=$const.

System	Fixed parameter	Boundary condition	Linear fit for $D_{\mathcal{L}}$	rms error of fit	Linear fit for Σ^+	rms error of fit
BE	$N=500$	Periodic	$-1.499+128.9/\sqrt{D}$	0.2421	$-0.06705+3.818/\sqrt{D}$	0.007420
BE	$D=16$	Periodic	$-0.2175+0.06151N$	0.03850	$-0.02241+0.001807N$	0.002020
BE	$\frac{N}{\sqrt{D}}=250$	Periodic	62.15	0.7946	1.813	0.02769
WS	$D=0.25$	No flux	$0.9767+0.03539N$	0.3115	$0.001189+1.791\times10^{-5}N$	0.0003796
WS	$D=0.25$	Periodic	$0.2272+0.03606N$	0.2304	$0.0001183+1.890\times10^{-5}N$	0.0003587
WS	$\frac{N}{\sqrt{D}}=2000$	Periodic	36.99	0.6054	0.02022	0.001271
GS, $\mu=33.5$	$N=500$	Periodic	$-0.05447+130.5/\sqrt{D}$	0.01766	$-0.03049+2.872/\sqrt{D}$	0.004593
GS, $\mu=33.5$	$D=16$	Periodic	$-0.1074+0.06540N$	0.02012	$-0.01160+0.001393N$	0.002511
GS, $\mu=33.5$	$\frac{N}{\sqrt{D}}=250$	Periodic	65.05	0.2733	1.450	0.07389
GS, $\mu=33.7$	$N=500$	Periodic	$-0.07992+122.4/\sqrt{D}$	0.01723	$-0.01816+2.281/\sqrt{D}$	0.001831
GS, $\mu=33.7$	$D=16$	Periodic	$-0.1148+0.06125N$	0.02296	$-0.01462+0.001126N$	0.003871
GS, $\mu=33.7$	$\frac{N}{\sqrt{D}}=250$	Periodic	61.11	0.03848	1.138	0.04028
GS, $\mu=33.7$	$D=16$	No flux	$0.3643+0.06126N$	0.007197	$0.01095+0.001122N$	0.001092
GS, $\mu=33.7$	$D=16$	Shortcut, $k=50$	$-1.528+0.06121N$	0.02385	$-0.03057+0.001117N$	0.001562
GS, $\mu=33.7$	$D=16$	Shortcut, $k=N/2$	$-1.233+0.06124N$	0.02963	$-0.04299+0.001118N$	0.004419
GS, $\mu=33.9$	$N=500$	Periodic	$-0.08079+103.3/\sqrt{D}$	0.03807	$-0.01055+1.203/\sqrt{D}$	0.002227
GS, $\mu=33.9$	$D=16$	Periodic	$-0.1022+0.05175N$	0.01903	$-0.009298+0.0006021N$	0.001796
GS, $\mu=33.9$	$\frac{N}{\sqrt{D}}=250$	Periodic	51.63	0.07226	0.5970	0.01081

ing the escape rate [38]. Figure 5(c) and Table I show that Σ^+ is an extensive quantity for all three models with varying system parameters and boundary conditions.

The Gray-Scott system was simulated for four different boundary conditions: periodic, no-flux, periodic with an added shortcut in the network of length $k=50$ ($k \ll N$), and with an added shortcut of length $k=N/2$. Table I shows that the rate at which the Lyapunov dimension $D_{\mathcal{L}}$ (and also Σ^+) increases with the network size N is rather independent of these boundary conditions, but their Y intercepts are significantly different for different boundary conditions. This is consistent with the finding in Sec. III for the rate at which the average transient lifetimes $\langle T \rangle$ increase with N. For a fixed network size, Fig. 2 and Table I reveal that $\langle T \rangle$, $D_{\mathcal{L}}$, and Σ^+ are largest for no-flux boundary conditions, second largest for periodic boundary conditions, and third largest for the presence of a shortcut in the network. There are, however, differences in the rankings for $\langle T \rangle$, $D_{\mathcal{L}}$, and Σ^+ for the two different types of shortcut length.

In the following we present a qualitative argument for why the linear fit of Lyapunov dimension $D_{\mathcal{L}}$ vs network size N has nearly zero Y intercept for all systems with periodic boundary conditions, as seen from Fig. 5(a) and Table I. If we assume that subsystems in reaction-diffusion networks do not interact across large distances, the Lyapunov dimension should not be affected by transformations that alter the global topology but conserve the local network structure and the total number of nodes. Figure 6 shows such a transformation that turns two networks of N nodes into one network of $2N$ nodes. Since the Lyapunov dimension is additive among nonconnected systems we expect that $D_{\mathcal{L}}(2N)=2D_{\mathcal{L}}(N)$. Together with the linear ansatz, $D_{\mathcal{L}}=aN+b$, it follows that $b=0$. This indicates that the Lyapunov dimension for very large system sizes and long simulation times follow a linear law with zero intercept. For systems with no-flux boundary conditions this line of reasoning is not valid since two such systems cannot be combined into one without changing the local structure (i.e., two of the no-flux boundaries would have to be removed).

For a ring network we also vary the coupling parameter D while keeping the network size N fixed. We find that the Lyapunov dimension $D_{\mathcal{L}}$ as well as the sum of positive Lyapunov exponents Σ^+ increases linearly with $1/\sqrt{D}$ for all three reaction-diffusion networks and various system parameters (Table I).

The general characteristics of the reaction-diffusion networks in Eq. (1) are conserved if N and D vary such that $N/\sqrt{D}$ is fixed (Sec. II). Table I shows that in this case $D_{\mathcal{L}}$ as well as Σ^+ are constant for a wide range of N and D values.

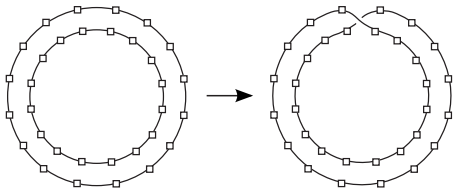

FIG. 6. A transformation that turns two ring networks each having N nodes into one network with $2N$ nodes, without changing the local network structure or the total number of nodes.

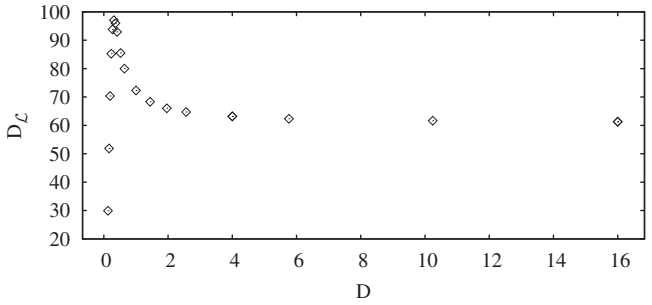

FIG. 7. Lyapunov dimension $D_{\mathcal{L}}$ vs coupling constant D for the Bär-Eiswirth ring network (α=0.84, β=0.07, and ϵ=0.12). The effective system size was held constant by varying the number of nodes N according to $N/\sqrt{D}$=250. This system had particularly large deviations from constant $D_{\mathcal{L}}$ for small D.

Figure 7 also confirms for the Bär-Eiswirth model that the Lyapunov dimension is constant over a range of coupling parameters D, when $N/\sqrt{D}$ is fixed. Significant deviations from a constant Lyapunov dimension exist for small values of D, where the network model deviates significantly from the continuum model. $D_{\mathcal{L}}$ was about 58% higher when D =0.3136 compared to the regime of constant dimension (Fig. 7). Two simulations with different initial conditions were made for each of the coupling parameters, D=4 and 16, and the results are close enough that the difference between the two simulations is difficult to see on the graph in Fig. 7. For the Gray-Scott systems [with three different system parameters (Table I)] the Lyapunov dimension was constant (within 1.4%) for coupling parameters D even down to D=1, which is close to the point where the system can no longer support chaos ($D \approx 0.7$). The Wacker-Schöll system had a variation in $D_{\mathcal{L}}$ of about 4% and a variation in Σ^+ of about 19% over the range of coupling parameters, $0.04 \leq D \leq 0.25$, which are close to the value for which the system can no longer support chaos. The qualitative behavior of Σ^+ was similar to that of $D_{\mathcal{L}}$, but in general had larger relative variations.

The qualitative argument for why the range of D for which $D_{\mathcal{L}}$ and Σ^+ are constant is bounded from below for all three reaction-diffusion networks follows from the excitability property. If D is low enough, the coupling term in Eq. (1) can no longer provide superthreshold perturbations to perturb the system away from the stable rest state and sustain spatiotemporal chaos.

V. CHAOTIC SADDLE AS QUASIATTRACTOR

Hunt *et al.* conjectured a formula for computing the dimension of the stable and unstable manifolds (D_s, D_u) of a chaotic saddle based on the Lyapunov spectrum and escape rate [37]. In the case of very low escape rate their formula reduces to [17]

$$D_s = 2N - \frac{\kappa}{\lambda_1},$$

$$D_u = D_{\mathcal{L}} - \frac{\kappa}{|\lambda_{j+1}|}, \tag{8}$$

where $2N$ is the dimension of the phase space, $\kappa = \langle T \rangle^{-1}$ is the escape rate, λ_1 is the largest Lyapunov exponent, $D_{\mathcal{L}}$ is the Lyapunov dimension, and j is the largest integer for which $\Sigma_{i=1}^{j} \lambda_i > 0$.

When the lifetime is long enough that the computation of the Lyapunov spectrum is feasible, the stable manifold has a dimension nearly equal to that of the entire phase space and the unstable manifold has a dimension nearly equal to the Lyapunov dimension of the saddle. For instance, in the case of the Wacker-Schöll ring network (α=0.02, τ=0.05, j_0 =1.21, d=8, D=0.25) with N=600 nodes, $\langle T \rangle = 4.19 \times 10^5$, λ_1=0.002 76, j=22, and with λ_{23}=−0.003 21, the stable and unstable manifolds of the chaotic saddle have dimensions

$$D_s = 2N - 0.000\ 865,$$

$$D_u = D_{\mathcal{L}} - 0.000\ 744, \quad \text{with } D_{\mathcal{L}} = 22.02 \pm 0.14.$$

The uncertainty due to convergence of $D_{\mathcal{L}}$ is approximately 0.14, which is more than two orders of magnitude larger than the corrections. As $N \to \infty$ we have $\kappa \to 0$ and so $D_s \to 2N$ and $D_u \to D_{\mathcal{L}}$.

For the Bär-Eiswirth ring network (α=0.84, β =0.07, ϵ=0.12, D=16) with N=400 nodes, $\langle T \rangle = 7.01 \times 10^5$, λ_1=0.131, j=24, and with λ_{25}=−0.129, the dimensions of the stable and unstable manifolds are

$$D_s = 2N - 0.000\ 010\ 9,$$

$$D_u = D_{\mathcal{L}} - 0.000\ 011\ 1, \quad \text{with } D_{\mathcal{L}} = 24.386 \pm 0.053.$$

For the Gray-Scott ring network (μ=33.7, Φ=2.8, D =16) with N=200 nodes, $\langle T \rangle = 1.64 \times 10^6$, λ_1=0.0792, j =12, and with λ_{13}=−0.107, the dimensions of the stable and unstable manifolds are

$$D_s = 2N - 0.000\ 007\ 70,$$

$$D_u = D_{\mathcal{L}} - 0.000\ 005\ 68, \quad \text{with } D_{\mathcal{L}} = 12.124 \pm 0.012.$$

Following the argumentation by Tél and Lai [17], the chaotic saddle behaves like a quasiattractor for all three models, since the unstable manifold of the chaotic saddle has nearly the same dimension as the saddle ($D_u \approx D_{\mathcal{L}}$), and since the stable manifold is nearly space filling, i.e., the stable manifold nearly forms a basin of attraction for the quasiattractor. In addition, the dimension of the chaotic saddle is very close to the dimension of an attractor with the same Lyapunov spectrum [17].

VI. INTENSIVE QUANTITIES

Densities can be defined from the extensive quantities $D_{\mathcal{L}}$ and $\ln\langle T \rangle$. The *(Lyapunov) dimension density* (δ_D) is given by

$$\delta_D = \lim_{N \to \infty} N^{-1} D_{\mathcal{L}}, \tag{9}$$

which describes the number of active degrees of freedom per unit volume [15]. Likewise, *the logarithmic-lifetime density* δ_T is defined as

TABLE II. Logarithmic-lifetime density δ_T and Lyapunov dimension density δ_D for the BE model ($\alpha=0.84$, $\beta=0.07$, $\epsilon=0.12$, $D=16$), the GS model ($\mu=33.7$, $\Phi=2.8$, $D=16$), and the WS model ($\alpha=0.02$, $\tau=0.05$, $j_0=1.21$, $d=8$, $D=0.25$) for different boundary conditions. Points were only considered for the linear fit if they were within the range of N for which $\langle T\rangle$ was consistently larger than the cutoff value.

System	Cutoff	Boundary condition	δ_D	δ_T	$\sigma=\delta_T/\delta_D$
BE	10^4	Periodic	0.0615	0.0309	0.502
GS	10^4	No flux	0.0613	0.0685	1.12
GS	10^4	Periodic	0.0613	0.0831	1.36
GS	10^4	Shortcut, $k=50$	0.0612	0.0818	1.34
GS	10^4	Shortcut, $k=N/2$	0.0612	0.0820	1.34
WS	10^4	No flux	0.0354	0.00632	0.179
WS	10^4	Periodic	0.0361	0.00689	0.191
BE	10^5	Periodic	0.0615	0.0292	0.474
GS	10^5	No flux	0.0613	0.0718	1.17
GS	10^5	Periodic	0.0613	0.0788	1.29
GS	10^5	Shortcut, $k=50$	0.0612	0.0839	1.37
GS	10^5	Shortcut, $k=N/2$	0.0612	0.0757	1.24
WS	10^5	No flux	0.0354	0.00613	0.173
WS	10^5	Periodic	0.0361	0.00576	0.160

$$\delta_T = \lim_{N\to\infty} N^{-1} \ln\langle T\rangle. \tag{10}$$

From Sec. V it follows that the *dimension density of the stable manifold of the chaotic saddle* [17], $\delta_s=D_s/N$, is about $d=2$ for all our model systems since $D_s\approx 2N$ in Eq. (8) with $2N$ as the dimension of the phase space and with $d=2$ as the dimension of the uncoupled dynamical system in Eq. (1). The *dimension density of the unstable manifold of the chaotic saddle*, $\delta_u=D_u/N$, is about $\delta_u=\delta_D$ since $D_u\approx D_{\mathcal{L}}$ for all our model systems. Due to these similarities we focus on the dimension of the chaotic saddle (δ_D) in the following.

Table II shows that the dimension densities are rather small for the chaotic saddle in all model systems, reflecting a low degree of freedom per network node. This is consistent with an earlier study by Strain and Greenside [2] for the Bär-Eiswirth model in two spatial dimensions. Table II also reveals that the dimension density δ_D does not depend on the boundary condition. The logarithmic-lifetime density δ_T is also rather low for all model systems with a dependence on boundary conditions that appears to decrease as $N\to\infty$.

We qualitatively relate the densities to properties of the weakly coupled subsystems in extensive transient spatiotemporal chaos. The exponential scaling of the average lifetime with the network size (type-II supertransients [17]) can be qualitatively explained by assuming weakly interacting correlated units of length ξ, with ξ approximately equal to the correlation length of the system. At any moment of time each of these units is conducive to loss of chaos with probability P. Spatiotemporal chaos collapses when all units are in such a conducive state [17], which happens with probability $P^{N/\xi}$. The lifetime takes the form

$$\langle T\rangle \sim P^{-N/\xi} = e^{-(\ln P)(N/\xi)}. \tag{11}$$

With Eq. (10) it follows that

$$\delta_T = \frac{-\ln P}{\xi} \tag{12}$$

for finite N. δ_T can now be interpreted as having units of number of coin tosses per unit length ξ. δ_T has the advantage of being a single computable quantity [from Eq. (10)], whereas the intuitive argument uses two quantities, ξ and P, both of which are open to interpretation. The ratio (σ) of these densities

$$\sigma = \delta_T/\delta_D \tag{13}$$

defines an intensive quantity that depends neither on the network size N nor on the coupling constant D since $\langle T\rangle$ as well as $D_{\mathcal{L}}$ is proportional to $N/\sqrt{D}$ from Sec. IV. If δ_T is interpreted as having units of number of coin tosses per unit length and δ_D is interpreted as being the number of active degrees of freedom per unit length, then σ has units of number of coin tosses per active degree of freedom. This quantity is significant because it is intensive and independent of the coupling strength, and thus suggests that transient spatiotemporal chaos in reaction-diffusion networks with homogeneous network structure can be understood from its local dynamics.

Combining Eqs. (10) and (13) to

$$\langle T\rangle^{-1} = e^{-\sigma D_{\mathcal{L}}} = (e^{-\sigma})^{D_{\mathcal{L}}} \tag{14}$$

leads to an intuitive argument for the escape rate from the chaotic saddle in the limit $N\to\infty$ if we assume that σ is given. Equation (14) can be interpreted as the volume of a hypercube of width $e^{-\sigma}$, if we ignore that the dimension of the chaotic saddle is fractal, and if we ignore that $D_{\mathcal{L}}$ is only approximately the fractal dimension. This hypercube can be considered as a hole in the chaotic saddle through which a trajectory can escape into a nonchaotic state. Larger systems have an attractor which resembles a set product of smaller

systems, and the escape hole resembles a set product of identical low-dimensional boxes with edges that have a geometric mean of $e^{-\sigma}$.

VII. CONCLUSIONS

A systematic study reveals that transient spatiotemporal chaos is extensive in three reaction-diffusion networks with various boundary conditions. The Lyapunov dimension, the sum of positive Lyapunov exponents, and the logarithm of the transient lifetime grow linearly with the system size. This indicates that even in the case of transient dynamics the larger systems act as if they were comprised of weakly interacting and statistically similar subsystems, with no new collective phenomena arising when such subsystems connect together. This might open up the possibility for modeling transient spatiotemporal chaos with statistical mechanics [13].

The effective system size for a network with N nodes and coupling parameter D is determined by $N/\sqrt{D}$. For a wide variety of coupling parameters and network sizes the number of active degrees of freedom (expressed in the Lyapunov dimension) stays constant as long as the effective system size is fixed. An upper bound for the entropy (expressed by the sum of positive Lyapunov exponents) is also constant for a fixed effective system size. Unless the coupling parameter D is sufficiently small, the network model approaches the continuum model.

The spontaneous collapse of spatiotemporal chaos points to the coexistence of a chaotic saddle with the regular attractor(s). Applying the dimension formulas of Hunt *et al.* [37], we find for all three models that the dimension of the unstable manifold of the chaotic saddle is nearly the dimension of the chaotic saddle, and the stable manifold of the chaotic saddle is nearly space filling. Thus, the chaotic saddle behaves like a quasiattractor according to Tél and Lai [17].

For extensive transient spatiotemporal chaos a dimension density and a logarithmic-lifetime density can be defined. A qualitative argument relates the escape rate from the chaotic saddle to a hole through which a trajectory can escape into a nonchaotic state. This hole has the form of a hyper-rectangle; its dimension is the Lyapunov dimension, and its width is determined by the ratio of logarithmic-lifetime and dimension densities.

The boundary conditions seemingly do not affect the dimension and logarithmic-lifetime densities, but do affect the x intercepts of the graphs of Lyapunov dimension versus network size and logarithmic-lifetime versus network size. It would be interesting to study whether the choice of boundary conditions shifts both the Lyapunov dimension and the logarithmic-lifetime graphs by the same number of nodes. In this case boundary conditions would change the effective network size. Unfortunately, since the computation time required to compute the average lifetime grows exponentially with the network size, the range of network sizes that are currently computationally accessible by supercomputers is not sufficient to determine the offset for different boundary conditions accurately enough because the slopes converge slowly.

ACKNOWLEDGMENTS

This research is based upon work supported by the National Science Foundation under Grant No. PHY-0653086, and by the Arctic Region Supercomputing Center at the University of Alaska Fairbanks as part of the Department of Defense High Performance Computing Modernization Program.

[1] A. Wacker, S. Bose, and E. Schöll, EPL **31**, 257 (1995).
[2] M. C. Strain and H. S. Greenside, Phys. Rev. Lett. **80**, 2306 (1998).
[3] R. Wackerbauer and K. Showalter, Phys. Rev. Lett. **91**, 174103 (2003).
[4] G. Huber, P. Alstrom, and T. Bohr, Phys. Rev. Lett. **69**, 2380 (1992).
[5] R. Braun and F. Feudel, Phys. Rev. E **53**, 6562 (1996).
[6] F. H. Willeboordse, Phys. Rev. E **47**, 1419 (1993).
[7] Y.-Ch. Lai and R. L. Winslow, Phys. Rev. Lett. **74**, 5208 (1995).
[8] B. Hof, J. Westerweel, T. M. Schneider, and B. Eckhardt, Nature (London) **443**, 59 (2006).
[9] A. Politi, R. Livi, G. L. Oppo, and R. Kapral, EPL **22**, 571 (1993).
[10] D. Ruelle, Commun. Math. Phys. **87**, 287 (1982).
[11] D. Ruelle, *Chaotic Evolution and Strange Attractors* (Cambridge University Press, New York, 1989).
[12] M. C. Cross and P. C. Hohenberg, Rev. Mod. Phys. **65**, 851 (1993).
[13] M. P. Fishman and D. A. Egolf, Phys. Rev. Lett. **96**, 054103 (2006).
[14] S. Tajima and H. S. Greenside, Phys. Rev. E **66**, 017205 (2002).
[15] H. Greenside, *Spatiotemporal Chaos in Large Systems: The Scaling of Complexity With Size*, CRM Proceedings and Lecture Notes Vol. 20 (Kluwer Academic, Secaucus, NJ, 1999), p. 9.
[16] S. Ruffo, *Lyapunov Spectra in Spatially Extended Systems* (The Erwin Schrödinger International Institute for Mathematical Physics, Vienna, 1997); *Cellular Automata and Complex Systems (Santiago, 1996)* (American Mathematical Society, Providence, RI, 1999), pp. 153–180.
[17] T. Tél and Y. C. Lai, Phys. Rep. **460**, 245 (2008).
[18] R. Wackerbauer, Phys. Rev. E **76**, 056207 (2007).
[19] R. Wackerbauer and S. Kobayashi, Phys. Rev. E **75**, 066209 (2007).
[20] J. P. Crutchfield and K. Kaneko, Phys. Rev. Lett. **60**, 2715 (1988).
[21] P. Gray and S. K. Scott, Chem. Eng. Sci. **39**, 1087 (1984).
[22] M. Bär and M. Eiswirth, Phys. Rev. E **48**, R1635 (1993).
[23] J. H. Merkin, V. Petrov, S. K. Scott, and K. Showalter, Phys. Rev. Lett. **76**, 546 (1996).
[24] M. G. Zimmermann, S. O. Firle, M. A. Natiello, M. Hilde-

brand, M. Eiswirth, M. Bär, A. K. Bangia, and I. G. Kevrekidis, Physica D **110**, 92 (1997).
[25] M. Or-Guil, J. Krishnan, I. G. Kevrekidis, and M. Bär, Phys. Rev. E **64**, 046212 (2001).
[26] M. Meixner, S. Bose, and E. Schöll, Physica D **109**, 128 (1997).
[27] The temporal period d_t and the spatial period d_i were defined as $x(i+d_i,t+d_t)=x(i,t)$. A two-dimensional autocorrelation analysis for the patterns in Figs. 1(c)–1(e) yields a temporal period of $d_t=712.0$ and $d_i=0.0$ for (c), $d_t=702.2$ and $d_i=-7.4$ for (d), and $d_t=969.8$ and $d_i=-24.5$ for (e). In comparison the period of the limit cycle for the uncoupled WS system is $d_t=257.6$.
[28] G. Benettin, L. Galgani, and J. M. Strelcyn, Phys. Rev. A **14**, 2338 (1976).
[29] This method determines the lifetime with sufficient accuracy, assuming that the maximum Lyapunov exponent is positive on average during the chaotic transient dynamics and zero on average during the nonchaotic dynamics, which is the case when the attractor is not a fixed point. All simulations for the Wacker-Schöll system fulfilled this criterion.
[30] S. Yonker and R. Wackerbauer, Phys. Rev. E **73**, 026218 (2006).
[31] In the Gray-Scott system the probability for local extinction could be associated with the probability P of a unit to be conducive to collapse. Test simulations show that no-flux boundary conditions as well as shortcuts in the network change locally the probability for local extinctions.
[32] Transient spatiotemporal chaos can become asymptotic for a constant boundary condition that provides a superthreshold perturbation to the excitable reaction-diffusion network [3].
[33] T. S. Parker and L. O. Chua, *Practical Numerical Algorithms for Chaotic Systems* (Springer-Verlag, Berlin, 1989).
[34] Computation of Lyapunov exponents can be sensitive to integration time step and time between renormalizations [14]. One representative system for each of the three models (Gray-Scott, Bär-Eiswirth, and Wacker-Schöll) was run with an integration time step five times smaller and then with a renormalization interval five times shorter. In all cases the difference in either Lyapunov dimension or sum of positive Lyapunov exponents between the trial and the baseline cases was less than 1.8 times the estimated convergence error.
[35] Runs that survived for a time less than $5\times10^6\Delta t$ were discarded under the assumption that not enough data would be available to get a reliable value for the Lyapunov exponents. Additionally, each system is run to time $10\,000\Delta t$ before perturbation vectors are followed to minimize the significance of the initial period before the chaotic saddle has been reached, and the perturbation vector data gathered in the first 4500 time units were discarded in order to allow the vectors to align in a natural way.
[36] E. Ott, *Chaos in Dynamical Systems* (Cambridge University Press, Cambridge, England, 2002).
[37] B. R. Hunt, E. Ott, and J. A. Yorke, Phys. Rev. E **54**, 4819 (1996).
[38] T. Tel, in *Transient Chaos*, Directions in Chaos Vol. 3, edited by B.-L. Hao (World Scientific, Singapore, 1990).